

The Structure of Thermohaline and Bio-Optical Fields in the Surface Layer of the Kara Sea in September 2011

P. O. Zavialov, A. S. Izhitskiy, A. A. Osadchiev, V. V. Pelevin, and A. B. Grabovskiy

Shirshov Institute of Oceanology, Russian Academy of Sciences, Moscow, Russia

e-mail: peter@ocean.ru

Received June 3, 2013; in final form, July 1, 2013

Abstract—We present data of measurements of thermohaline and bio-optical fields in the surface layer of the Kara Sea carried out in September 2012, during the 59th cruise of the R.V *Akademik Mstislav Keldysh*. Measurements were performed during vessel motion along the expedition route using a pump-through CTD system (temperature and salinity) and UV fluorescent lidar (concentrations of chlorophyll, total suspended matter, and dissolved organic matter) with a high spatial resolution (about 10–100 m). Detailed sea-area distribution maps of the above parameters are presented, frontal zones are detected, T,S diagrams for the surface water layer are constructed, and basic water types are identified. It is shown that Ob–Yenisei freshwater runoff is a main factor affecting properties of the surface layer. In the second part of this paper, a numerical model of the dynamics of continental runoff in the Kara Sea is suggested. Model experiments were carried out under real wind conditions of August–September 2011 (NCAR/NCEP reanalysis); the model was validated on the basis of in situ data collected during the cruise.

DOI: 10.1134/S0001437015040177

INTRODUCTION

Geographical maps allow one to assume that properties of Kara Sea waters are decisively determined by the interaction of three water mass types significantly different in origin and parameters: Barents Sea waters, which arrive from the west through the Kara Strait; Arctic Basin waters, which invade from the north near the St. Anna Trench to the east of Novaya Zemlya; and freshwater runoff from Ob and Yenisei estuaries. Continental waters are very important for the surface sea layer; the character of their propagation over the seawater area is characterized by significant interannual variability and is determined by both magnitude and variability of river runoff and wind effects [3, 11; see also Zatsepin et al., 2015 in this issue *Oceanology*].

The rivers bring about 1350 km³ of freshwater per year on the average to the Kara Sea [2] (let us note here that the annual average Danube runoff to the Black Sea is “only” 200 km³, and the Volga runoff to the Caspian Sea is about 250 km³). Annual average river runoff to the Kara Sea over its water area is a layer of 152 cm in depth [5]. This is a very significant volume of freshwater, which accumulate their own heat and momentum, carry suspended matter, dissolved organic matter, and biogenic matters; it propagates over a wide territory in a comparatively shallow basin and significantly affects all Kara Sea systems. The runoff effect is not reducible to just the direct exchange of properties between mixing river water and seawater. Dynamic effects are of an equivalent importance; they are connected with the capability of runoff to form high-

power density stratification in the surface sea layer and thus suppressing vertical mixing and “screening” the lower water layers from heat and momentum exchange with the atmosphere. Regularities of continental water transport to the sea under wind effect and sea currents under conditions of interaction with surrounding water masses have been insufficiently studied.

Hydrological and hydrophysical researches of the modern Kara Sea are of great interest in the context of climate change in marginal Arctic seas. However, the Kara Sea remains the least studied, and data on this sea are the poorest. In view of the diversified character of hydrophysical processes in the Kara Sea and the difficult accessibility of this part of the ocean for remote sounding due to permanent cloud cover, we may suggest complex expedition studies as a main method for the investigation of the Kara Sea. Such studies were carried out during the 59th cruise of the RV *Akademik Mstislav Keldysh* in September–October 2011.

In this work, we describe the results of that expedition as regards the measurement of thermohaline and the bio-optical parameters of the sea surface layer. On the basis of this data, we analyze the spatial distribution of hydrological fields over the seawater area, determine frontal zones and main water masses, and discuss qualitative parameters of water mass mixing. To interpret the thermohaline structure of the sea surface layer, we present a numerical model developed to reproduce continental runoff to the sea and apply it for conditions that correspond to the expedition period.

MEASURING EQUIPMENT AND TECHNIQUE

During the cruise, the thermohaline parameters of the sea surface layer were monitored during vessel motion with a pump-through CTD system. The water was sampled with a vacuum centrifugal pump Grundfos JP-6 of 1.5 kW in power through a coiled flexible hose 9 m long, extended from the working deck. During vessel motion, the pump end of the hose was kept at a depth of 0.5–1 m under the water surface with a system of lead weights and braces. Pump capacity is 0.8 L/s. The water was supplied to a special closed container of 70 L in volume with a SeaBird SBE 911 CTD tool inside, which was fixed on the desk. The sounding data were transmitted via cable to a laboratory computer along with onboard GPS data. The primary measurement rate with the SBE911 tool was 24 measurements per second at a GPS sampling rate of 2 Hz. Water-renewal time in the container was about 100 s. This corresponds to a spatial scale of data “smoothing” of about 500 m at a vessel velocity of 10 kt.

During vessel motion, the sea surface was remotely sounded with a UFL-9 fluorescent scanning lidar. This lidar is intended for express measurements of seawater concentrations of dissolved organic matter, phytoplankton chlorophyll, and suspended matter. The main specifications of the lidar are the following: laser wavelength is 354 nm, sounding frequency is 2 Hz, pulse energy is 2 mJ, sounding pulse length is 10 ns, input aperture of the receiver is 140 mm, 11 spectral channels. The lidar was mounted in the breast part of the vessel at the starboard shear of the erection deck, 7.5 m above the sea surface. A sounding beam was directed to the water surface at an angle of 45° into a surface water region free of foam. A UV laser pulse penetrates to a depth of 1–3 m and induces fluorescence of organic matter dissolved in this water column or on the surface and Raman scattered by the water. Laser and fluorescence radiation in the 354–685 nm range are accepted and analyzed by a spectrum-analysis unit of the lidar. Radiation intensities in different segments of this spectral range are then recalculated to concentrations of chlorophyll, suspended matter, and organic matter according to the techniques [1, 6].

Seawater was also sampled at stations and at certain points en route; samples were then filtered and preserved. One of the aims of the sampling was to measure the total seston concentration in weight units for the following comparison with lidar optical data. The samples were taken with a bucket. The filtering was carried out through Whatman CF/F fiber glass filters (pore size is 0.7 μm) and nuclear membrane filters (pore size is 0.45 μm).

DATA ANALYSIS

Horizontal distributions of the salinity and temperature on the Kara Sea water surface were constructed in sufficient detail on the basis of pump-through CTD system data for September–early October 2011 (Figs. 1a and 1b).

The data presented allow conventional contouring of desalinated surface waters. In our opinion, 19-PSU isohaline is the most appropriate for this. In view of this assumption, a fresh water plume eastward propagated from the Yenisei coast in a narrow band, and in a wider band, to the central part of the sea approaching the northern tip of Novaya Zemlya. It should be noted that this region significantly differed from the corresponding fresh water plume observed there in September 2007. In that case, the plume consisted of two separate parts: one part was located near the estuary, and another isolated part was near the central part of Novaya Zemlya [3]. Thus, the position, size, and state of fresh water plumes are strongly variable on scales from synoptic (see the next section) to interannual, connected, first of all, with the wind effect.

Several high-gradient zones can be distinguished, which demarcate different water masses in the sea surface layer (Fig. 1c):

(1) a front between Barents Sea waters to the east of the Kara Strait and water desalinated by continental runoff in the central part of the sea (F1 in Fig. 1c);

(2) a front between Arctic waters and waters desalinated by continental runoff near the southern tip of the Saint Anna Trench (F4 in Fig. 1c);

(3) an external Yenisei runoff estuarine front to the north of Sibiryakov Island and its continuation to the east near the Taymyr coast (F2 in Fig. 1c);

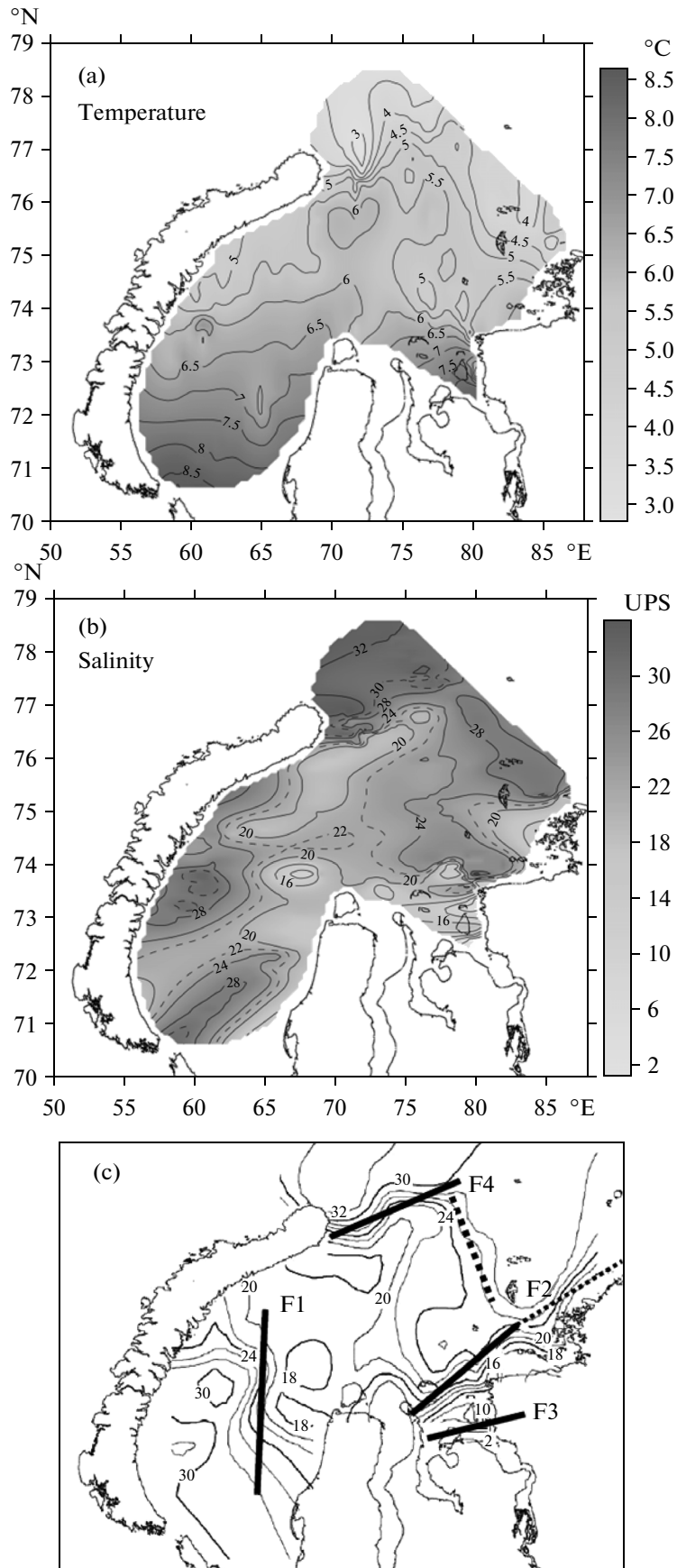
(4) an internal front of the Yenisei runoff within the Yenisei Bay to the south of Sibiryakov Island (F3 in Fig. 1c);

(5) a frontal zone that bounds the desalinated water region from the east and is elongated in the meridional direction from a region to the east of Saint Anna Trench toward Taymyr (heavy dashed curve in Fig. 1c).

The observed thermohaline structure of the sea surface layer can be generally characterized by a common T,S diagram constructed from all available data of the pump-through CTD system (20484 points in total).

We should note that T,S analysis is usually used for conservative ocean water masses and, generally speaking, is not applicable in cases where properties of such masses change due to not only their mutual mixing but also under effects of other external factors, e.g., heating of the upper sea layer with solar radiation. However, we can consider a general T,S diagram of the surface layer (Fig. 2) in such cases also. If thermohaline properties change significantly due to atmospheric

Fig. 1. Distributions of (a) temperature (°C) and (b) salinity (UPS) over the Kara Sea surface in September–October 2011; (c) schematic view of frontal zones selected on the background of surface salinity isolines (UPS).



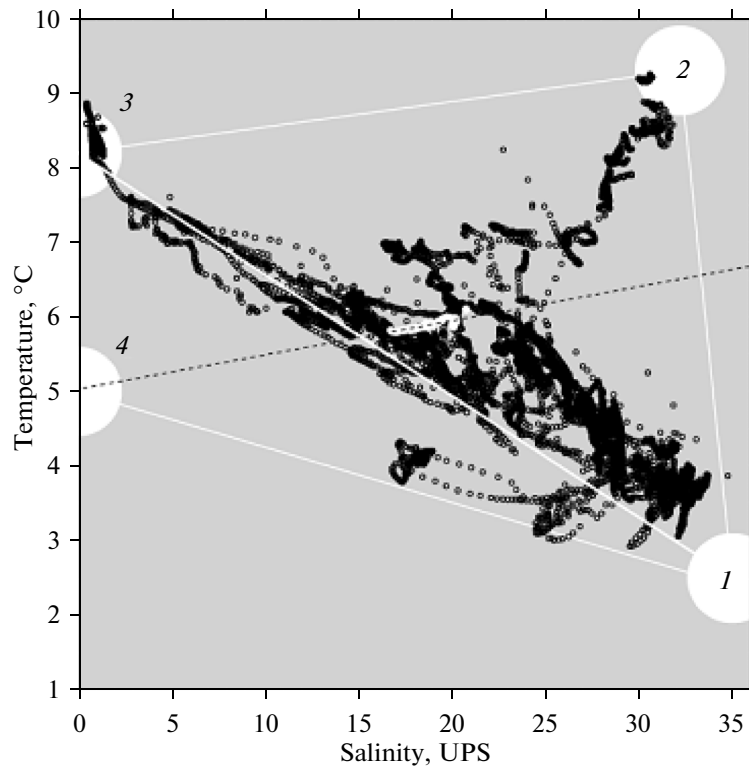


Fig. 2. General T,S diagram of Kara Sea surface waters in September–October 2011 and main water types: Arctic surface waters (1), Barents Sea waters (2), Yenisei runoff (3), Ob runoff (probably) (4). The region shown by white color in the center of the diagram corresponds to the vessel path segment the closest to the Ob estuary.

exchange processes, and mixing water temperature changes with time, then one can expect that the diagram is a cloud of points without an obvious arrangement. Linear structures are to be disturbed in it, and visible structures are to be projected into different temperature ranges on the axis corresponding to zero salinity. The diagram differs significantly in this case, and we want to attract the attention of readers to this fact.

One can see that T,S analysis points out the interaction of the following three water types: (1) salt (34–35 PSU) and cold (temperature $< 3.5^{\circ}\text{C}$) Arctic water, which arrives from the St. Anna Trough region; (2) water of lower salinity (31–32 PSU) and warm (up to 9.5°C) in the western part of the sea, which evidently arrives from the Barents Sea from the Kara Strait; (3) Yenisei freshwater with a temperature of about 8°C ; (4) desalinated waters of another genesis, formed due to mixing of Arctic waters and river runoff, probably from the Ob river, which is much colder than Yenisei (5.5°C), found in a quite local region in the eastern part of the region under study. Unfortunately, type (4) can be connected with Ob river runoff only hypothetically, since no measurements were carried out in the Ob Bay during the expedition, and the water temperature in the Ob estuary remained unknown. One can note that Ob waters were actually colder than Yenisei waters, and the temperature was about 6°C during the

previous expedition in the Kara Sea in September 2007; however, this does not imply the same in 2011.

Another indirect but obvious argument for the assumption that water type (4) in Fig. 2 corresponds to Ob runoff is the following. Data that relate to a vessel path segment on September 17, 2011, which is the closest to the outer side of the Ob Bay, approximately from the northeastern tip of Belyi Island to the point to the north of Shokal'skii Island, are shown by white color in the central part of the T,S diagram. Since this region is close to the Ob estuary, one can expect that more or less admixture of Ob river waters should be present in this region in any case. Indeed, the corresponding data in the T,S diagram lie on a straight line (black dashed line in Fig. 2), which points to mixing with water type 4, which indirectly confirms our assumption. If it is true, then this means that the main part of the continental runoff, which participated in formation of the surface Kara sea layer in September 2011, belonged to the Yenisei (water type 3 in Fig. 2), while the portion of Ob runoff was much less and more localized.

As follows from the T,S diagram, almost the entire variety of water types in the sea surface layer is well described by the simple mixing of the above listed surface-water masses, which allows one to talk about the two-dimensionality of interactions that prevail here and only the secondary part of ocean–atmosphere

Fig. 3. Fractions (in percentage of volume) of the content of main water types in the composition of the Kara Sea surface layer in September–October 2011: (a) Arctic surface waters, (b) continental runoff, and (c) Barents Sea waters.

currents and vertical mixing in the water formation processes.

The fractions α_1 , α_2 , and α_3 of the main water types are easily calculatable for each point of the T, S diagram within the 1–2–3 triangle. For this, the following simplest equations are to be solved:

$$\begin{aligned}\alpha_1 T_1 + \alpha_2 T_2 + \alpha_3 T_3 &= T_0, \\ \alpha_1 S_1 + \alpha_2 S_2 + \alpha_3 S_3 &= S_0, \\ \alpha_1 + \alpha_2 + \alpha_3 &= 100\%,\end{aligned}\quad (1)$$

where T_0 and S_0 are the temperature and salinity, respectively, that correspond to a given point, T_i and S_i ($i = 1, 2, 3$) are the temperature and salinity of water of the i th main type. Numerical values for T_i and S_i are given above. The results of solution of Eqs. (1) are shown in Figs. 3a–3c for all points of the polygon.

It is seen that surface Arctic waters (Fig. 3a) arrive at the northeastern part to the Kara Sea, especially near Saint Anna Trench, where their content attains 90%. A relatively high content of these waters (above 60%) is noted along the eastern coast of the northern and central part of Novaya Zemlya, precisely where an isolated continental-runoff desalinated water plume was observed in September 2007 [3]. We should note that surface Arctic waters generally predominate in the composition of surface Kara Sea waters—their fraction is from 30 to 80% almost across the entire seawater area (except for regions adjacent to the river estuaries and the Kara Strait), and their total content is estimated to be 59% in the Kara Sea surface layer in September 2011. Continental runoff (Fig. 3b) was localized in a wide band from the Yenisei estuary to the northern tip of Novaya Zemlya. The amount of continental runoff attains 50% in this region, and its total content in the sea surface layer is 34%. Finally, Barents Sea waters (Fig. 3c) are almost completely localized in the western part of the Kara Sea, as their total content does not exceed 7%.

Figure 4 shows the distributions of the total suspended matter, chlorophyll, and dissolved organic matter from UV fluorescent lidar UFL-9 sounding data. It is seen in Fig. 4a that regions of increased concentrations of suspended particles (higher than the background values by 40–100%) were observed in the central part of the sea in a band from the river estuaries to the northern tip of Novaya Zemlya. The character of the suspension concentration distribution generally repeats features of the distribution of low-salinity waters caused by continental runoff (see Fig. 2b). Let us note that this can be considered as another indirect argument for the above assumption that the main contribution to the formation of continental-origin waters in the Kara Sea belongs to the Yenisei, but not to the

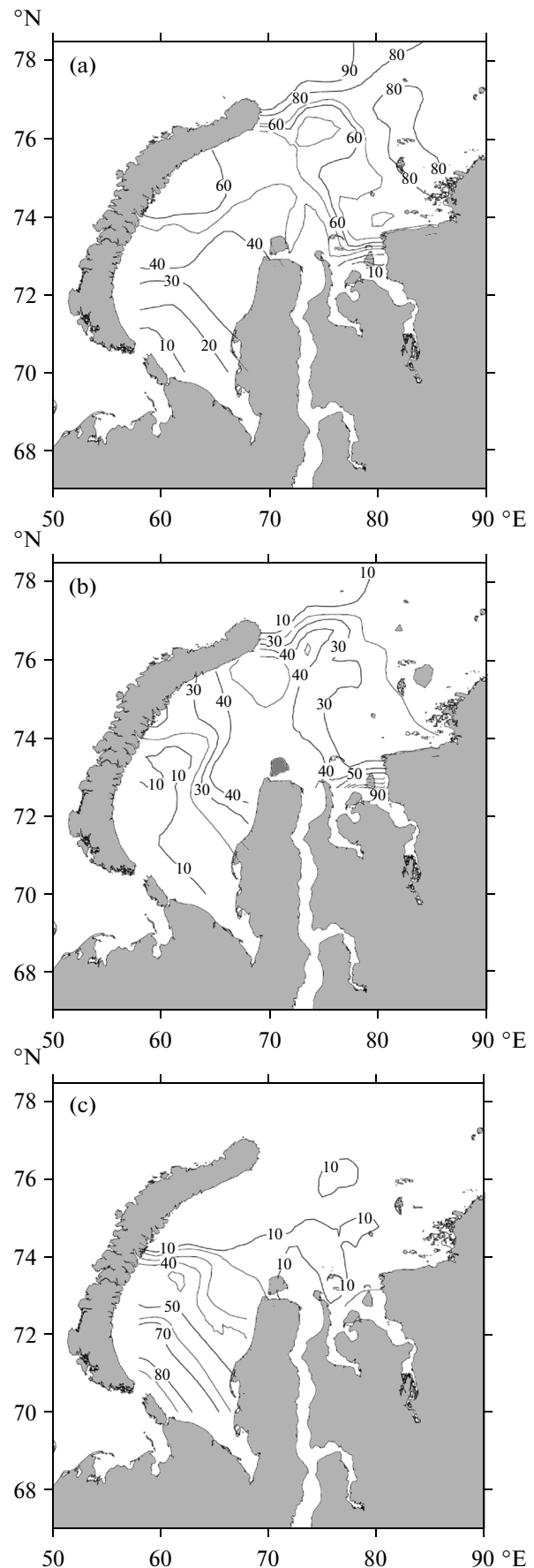


Fig. 4. Distributions of concentrations of (a) total suspended matter, (b) chlorophyll, and (c) dissolved organic matters over the Kara Sea surface in September–October 2011 from UV fluorescent lidar sounding data.

Ob River, in the period of observations. Indeed, as is known [4], the total suspended matter concentration in the Ob runoff is an order of magnitude lower than in the Yenisei runoff. Hence, Ob runoff should influence suspended-matter distribution comparatively less, even if it is clearly shown in a decrease in salinity. The distributions of chlorophyll (Fig. 4b) and dissolved organic matter concentrations (Fig. 4c) generally repeat the distribution of suspended-matter concentration, but they have some unique features. Thus, the chlorophyll concentration distribution is characterized by strong inhomogeneity: along with manifestations of river runoff effects, one can see maxima localized near the eastern coast of the central part of Novaya Zemlya; they might well be connected with the arrival of biogenic matter with coastal snowmelt runoff. The most oligotrophic regions with low chlorophyll concentrations can be noted in the western part of the sea in the region of predominance of Barents Sea waters arriving from the Kara Strait. A minimum of dissolved organic matter concentration is also observed there.

All the above ideas are based on the assumption that the above distribution of thermohaline and bio-optical fields are quasi-synoptic, i.e., they weakly vary with time over an almost one-month cruise. On the other hand, to ground the applicability of the T,S analysis at fixed values of salinity and temperature of main water types, they should mix quite rapidly, and the time variations in these parameters can be accounted. Thus, the question naturally arises about the characteristic time scales of variability of the Kara Sea surface layer in general and river runoff and desalinated water plumes in particular. The in situ observations carried out do not answer this question, and neither do satellite data (in view of the permanent thick clouds during the cruise, only several satellite images, at least those partly free of

clouds, are available for that period). Therefore, a numerical model is used in the next section, which has been developed for the description of motion of the Ob–Yenisei runoff-desalinated water plume under wind effect in October 2011.

NUMERICAL SIMULATION OF PROPAGATION OF RIVER RUNOFF AND DESALINATED WATERS

We use here a special numerical model of river-runoff propagation. The STRIPE (Surface-Trapped River Plume Evolution) was initially developed for the study of behavior of plumes of small rivers of the Russian coast of the Black Sea. However, it turned out later on that this approach can be used on larger scales. Below we briefly describe the model and features of its adaptation to the Kara Sea. The complete description of the model and its validation can be found in [10].

Model description. The model is based on the Lagrangian approach; it reproduces the motion of individual particles of river runoff under the action of hydrodynamic forces applied to them. Each particle is considered as a homogenous water column vertically extending from the surface to a river plume–seawater interface. The particles are emitted from river estuaries in certain time intervals with an assigned initial velocity, the module and direction of which may fluctuate near a specified mean value (proportional to the river runoff intensity) according to a homogeneous probability distribution. The number of particles emitted per unit time is also proportional to the runoff volume. The surface salinity and velocity fields can be constructed by means of interpolation of the corresponding values for individual particles to a regular grid at each step of model integration. The equations of motion for an individual particle have the form

$$\left. \begin{aligned} a_x^{i+1} &= f v^i + \frac{\tau_x^i}{\rho^i h^i} - \frac{\mu_v^i u^i - u_{sea}^i}{h^i} + \frac{\mu_h}{h^i} \left(\frac{u_{x+\Delta x,y}^i + u_{x-\Delta x,y}^i - 2u^i}{\Delta x} \right. \\ &\left. + \frac{u_{x,y+\Delta y}^i + u_{x,y-\Delta y}^i - 2u^i}{\Delta y} \right) - g \alpha \frac{h_{x+\Delta x,y}^i - h_{x-\Delta x,y}^i}{\Delta x}, \\ a_y^{i+1} &= -f u^i + \frac{\tau_y^i}{\rho^i h^i} - \frac{\mu_v^i v^i - v_{sea}^i}{h^i} + \frac{\mu_h}{h^i} \left(\frac{v_{x+\Delta x,y}^i + v_{x-\Delta x,y}^i - 2v^i}{\Delta x} \right. \\ &\left. + \frac{v_{x,y+\Delta y}^i + v_{x,y-\Delta y}^i - 2v^i}{\Delta y} \right) - g \alpha \frac{h_{x,y+\Delta y}^i - h_{x,y-\Delta y}^i}{\Delta y}, \end{aligned} \right\} \quad (2)$$

where the superscripts enumerate the model integration step; u , v , a_x , and a_y are the zonal and meridional components of the particle velocity and acceleration,

respectively; $(u_{x,y}, v_{x,y})$ are velocity components interpolated to a grid node with the coordinates (x, y) ; Δx and Δy are the grid steps in the zonal and meridi-

onal directions; f is the Coriolis parameter; (τ_x, τ_y) are the components of wind friction stress; ρ is the water density for the particle; h if the water column height in the particle, interpreted as the plume depth; $h_{x,y}$ is the plume depth interpolated to a grid node with the coordinates (x, y) ; μ_h and μ_v are the coefficients of vertical and horizontal turbulent friction; (u_{sea}, v_{sea}) are the zonal and meridional components of the current speed under the plume; g is the acceleration of gravity; and \aleph is the dimensionless scaling factor. In these equations, the first term in the right part corresponds to the Coriolis force acceleration, the second term, to the wind force applied to a particle, the third and fourth terms, to the vertical and horizontal frictions, respectively, and the last term, to the acceleration connected with a pressure gradient.

To consider small-scale horizontal turbulent mixing, Eqs. (2) are supplemented with the random walk scheme:

$$\left. \begin{aligned} x^{i+1} &= x^i + u^{i+1} \Delta t - \frac{a_x^{i+1} \Delta t^2}{2} + \sqrt{2D_h^i \Delta t} \eta_x, \\ y^{i+1} &= y^i + v^{i+1} \Delta t - \frac{a_y^{i+1} \Delta t^2}{2} + \sqrt{2D_h^i \Delta t} \eta_y, \end{aligned} \right\} \quad (3)$$

where (x, y) are the coordinates of a particle, Δt is the time step, D_h is the horizontal diffusion coefficient, and η_x and η_y are the independent normally distributed random variables implemented in the model with a random number generator. The time evolution of the density ρ and water salinity S for a particle is specified by the equation

$$\left. \begin{aligned} S^{i+1} &= S^i + \frac{D_v^i (S_{sea} - S^i)}{h_\tau h^i} \Delta t, \\ \rho^{i+1} &= \rho^i + \frac{D_v^i (\rho_{sea} - \rho^i)}{h_\tau h^i} \Delta t, \end{aligned} \right\} \quad (4)$$

where ρ_{sea} and S_{sea} are the sea water density and salinity under the plume, respectively, and h_τ is the vertical turbulence scale. The coefficient of horizontal and vertical diffusion used in the above equations have been calculated by the equations

$$D_h^i = \xi_h \Delta x \Delta y \sqrt{\left(\frac{u_{x+\Delta x, y}^i - u_{x-\Delta x, y}^i}{\Delta x} \right)^2 + \left(\frac{v_{x, y+\Delta y}^i - v_{x, y-\Delta y}^i}{\Delta y} \right)^2 + \frac{1}{2} \left(\frac{v_{x+\Delta x, y}^i - v_{x-\Delta x, y}^i}{\Delta x} + \frac{u_{x, y+\Delta y}^i - u_{x, y-\Delta y}^i}{\Delta y} \right)^2}, \quad (5)$$

$$\frac{D_v^i}{h_\tau} = \xi_v (1 - \min(1, Ri^i)^2)^3, \quad (6)$$

where ξ_h and ξ_v are the scaling factors, $Ri^i = \frac{N^i}{S^i}$ is the

Richardson number, $N^i = \frac{g \rho_{sea} - \rho^i}{\rho^i h_i}$ is the buoyancy

frequency, and $S^i = \frac{\sqrt{(u^i - u_{sea}^i)^2 + (v^i - v_{sea}^i)^2}}{h^i}$ is the

vertical velocity shift. Equation (5) is the well-known Smagorinsky formula [12], and Eq. (6) is taken from [8]. The following condition is used as boundary: if a particle reaches the coast, its velocity component normal to the coast becomes zero, while the tangential component remains invariable.

The STRIPE model was adapted to simulation of large-scale propagation of Ob and Yenisei runoffs in the Kara Sea. For simplification, it was decided to ignore details of desalinated water motion within the Ob and Tar Bays, as well as the Yenisei Bay. The model sources of continental runoff were located at the exits from the Ob and Yenisei Bays. NCAR/NCEP reanalysis fields for the region under study with a 6-hour time and 1-degree spatial resolutions were used as input wind data [7]. The Ob and Yenisei runoff powers were taken fixed and equal to the long-term averages for September [5]. Runoffs of Taz, Pyasina, and other smaller rivers flowing in the Kara Sea were ignored.

SIMULATION RESULTS

The propagation of Ob and Yenisei freshwaters from August 18 to October 5, 2011, was simulated with a resolution of 12 min. The initial configuration of the river plume was specified conventionally on the basis of a satellite map of chlorophyll concentration distribution on August 18. Simulation results were compared with several available satellite maps of chlorophyll and suspended matter concentration distributions, which are good markers of river runoff (August 21, September 4 and 8, 2011), and with in situ data measured during the cruise.

Such a comparison is exemplified in Fig. 5. It corresponds to September 23, 2011, when the vessel, going from the Arctic Institute Islands to the Taimyr coast, left seawater (salinity of about 28 PSU) and came into water desalinated by continental runoff (salinity of 17–18 PSU). In view of model salinity maps, the vessel path at that time also crossed the boundary of a plume propagated along the Taimyr coast. Both the model salinity in the desalinated water region and the position of the external boundary of the plume almost coincided with in situ data in that case.

Figure 6 shows positions of the Ob–Yenisei plume simulated for August 21, September 8 and 20, and October 4, 2011. Actual plume positions are shown schematically in the first two maps, which were estimated from satellite images of chlorophyll and suspended matter distributions. This and other compari-

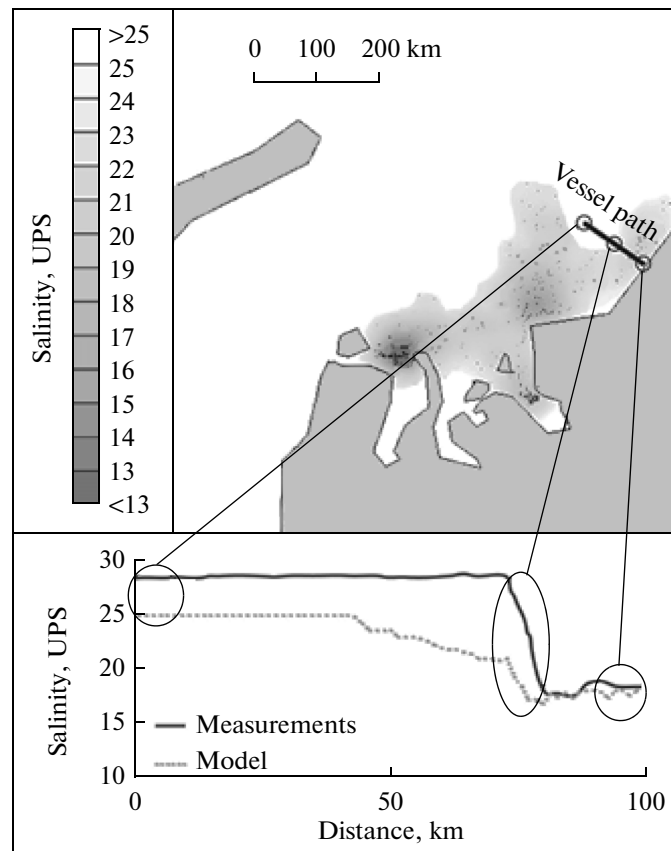


Fig. 5. (top) Position of the continental runoff–desalinated region simulated for September 23, 2011 (dashed curve) and the vessel path; (bottom) distributions of surface salinity along the vessel path from measurement results (solid curve) and simulation (dashed curve).

sons carried out witness that the model shows the plume position correctly in general, though omitting many details.

Simulation results allow one to judge the temporal variability of the freshwater region. According to calculations, the continental waters under the action of northeasters and northers were transported westward from the near-estuary regions to Novaya Zemlya in the second half of August. In that period, large sea areas between Yamal and eastern coast of Novaya Zemlya were in the region of Ob–Yenisei plume propagation.

Medium to strong southeasters predominated in the first half of September; they pressed the plume to the eastern coast of Novaya Zemlya, where it took the form of an isolated freshwater plume. At the same time, continental runoff formed a new quite large plume to the north of the river estuaries. The isolated plume part, which was between Yamal and Novaya Zemlya, completely dissipated by mid-September (Fig. 6c). The plume was displaced eastward and approached the Taimyr coast under the condition of dominant southwesterers and westerers by late September to early October (Fig. 6d).

Thus, simulation results show that the time scales on which the continental runoff–desalinated region

significantly changes location under a strong wind effect are comparable to or smaller than the time of expedition measurements. Unfortunately, this calls into doubt the possibility of considering the latter quasi-synoptic and hence too the distributions given in the first part of the work.

CONCLUSIONS

The structure of the thermohaline and bio-optical fields of the Kara Sea surface layer in September 2011 was determined by the interaction of the Ob–Yenisei runoff with surface Arctic waters arriving from the region of the St. Anna Trough and Barents Sea waters arriving through the Kara Strait. The ratios of these three water types were approximately 34 : 59 : 7 across the sea area (more exactly, across the part covered by expedition measurements). Almost the entire variety of water type in the sea surface layer was satisfactorily described by the linear mixing of these basic water masses; hence, surface layer dynamics was mainly two-dimensional. A similar pattern was observed during the expedition of 2007 [3].

The contact lines of the cores of the main surface water masses form frontal zones, which play a signifi-

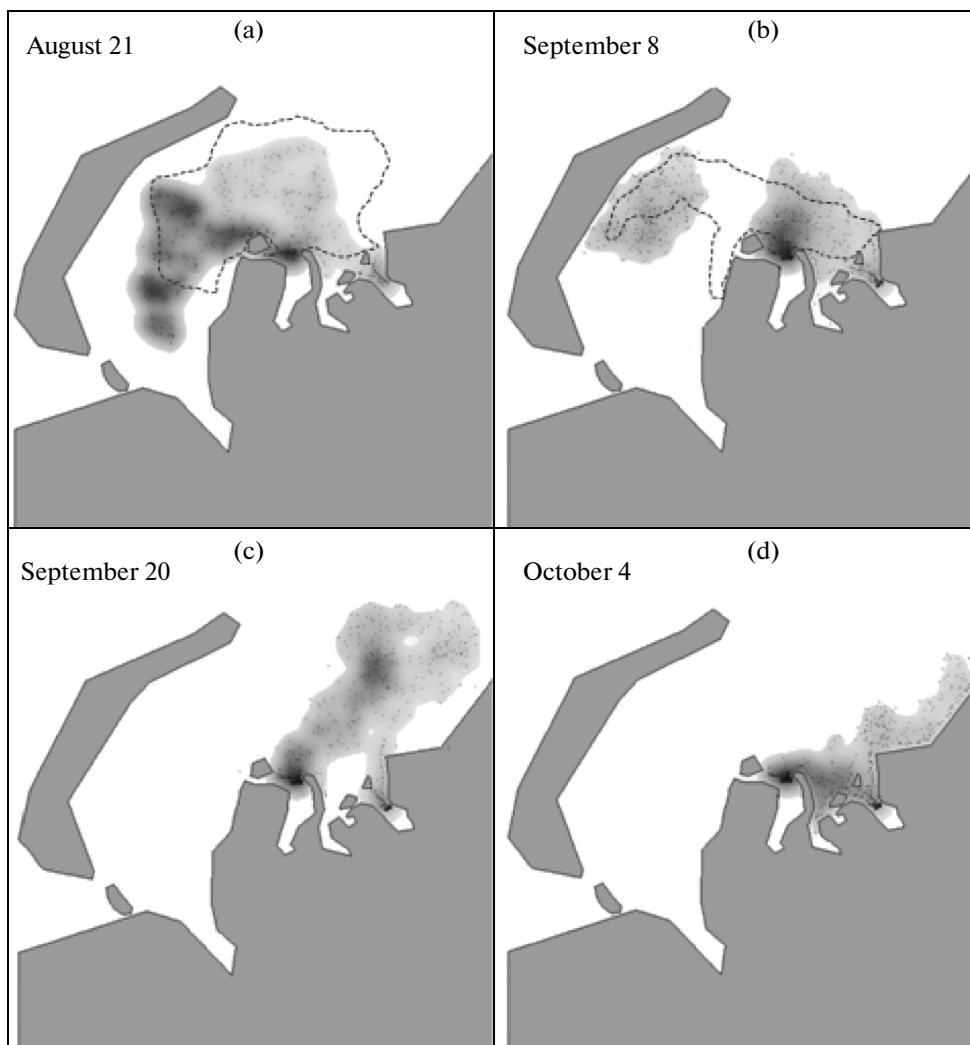


Fig. 6. Positions of the continental runoff–desalinated region simulated for (a) August 21, 2011, (b) September 8, 2011 (b), September 20, 2011 (c), and October 4, 2011 (d). Actual plume positions are shown in maps (a) and (b), estimated from satellite images of chlorophyll and suspended matter distributions.

cant role in functioning of many Kara Sea systems and the formation of its bioproductivity [see Flint et al., 2015 in this issue *Oceanology*]. We have selected five such zones from survey data of 2011.

T, S analysis shows that the main part in formation of continental-origin waters in the Kara Sea belonged to Yenisei runoff during the period under study. The Ob runoff is also clearly traceable but in a volume about an order of magnitude less than the Yenisei runoff volume and is spatially localized more clearly. However, the incompleteness of the data used (e.g., the absence of direct measurement of Ob runoff parameters) and some crucial restrictions of the method (e.g., assumptions about the steady thermohaline state of basic water types) do not allow us to consider the last statement as proved, but rather as a more or less grounded hypothesis.

It has been ascertained that the position of continental runoff–desalinated water plume, as well as its area and thermohaline parameters are strongly seasonally variable. The position and extent of the plume recorded during expedition measurement in 2011 differed significantly from those observed in 2007. In September 2007, the maximum desalination zone occupied an isolated region near the coast of the central part of Novaya Zemlya, while in September 2011, it formed a continuous band to the north and east of the river estuaries, whose periphery reached the northwestern tip of Novaya Zemlya and are the most clearly pronounced near the Taimyr coast. The absolute values of salinity in the plume in 2011 exceeded the values characteristic for 2007 by 1–3 UPS.

In our opinion, the variability of the Ob–Yenisei plume is determined by, first of all, wind effects. To study this mechanism, a specialized numerical model

was developed and applied to conditions in the Kara Sea in August–October 2011. Model experiments with the use of real data on wind (NCAR/NCEP reanalysis fields) allowed us to suggest a scenario of plume evolution during the period under study, which evidently did not contradict with the fragmentary data for certain time periods and with the few satellite images. According to this scenario, the desalinated water region in the early September 2011, had a form close to that of September 2007; however, during the expedition, it displaced eastward under the action of south-westerly winds and partly dissipated. This witnesses that the time scales of the variability of thermohaline and the bio-optical fields of the Kara Sea surface layer, at least in the region of continental runoff influence, can be smaller than is commonly accepted, and the expedition survey of the seawater area during 3–4 weeks can hardly be considered quasi-synoptic.

ACKNOWLEDGMENTS

We are grateful to D.M. Soloviev (Marine Hydrophysical Institute, Sevastopol) for satellite images provided.

The work was supported by the Ministry of Education and Science of the Russian Federation (three-part agreement no. 14.1325.31.0026, State Contract nos. 2042 and 8338), the Russian Foundation for Basic Research (project no. 13-05-00626), and CLIMSEAS project (International grant).

REFERENCES

1. N. A. Aibulatov, P. O. Zavialov, and V. V. Pelevin, "Hydrophysical self-purification of Russian coast of the Black Sea near the river estuaries," *Geoekologiya*, No. 4, 301–310 (2008).
2. A. D. Dobrovol'skii and B. S. Zalugin, *The Seas of the Soviet Union: Nature and Economics* (Mysl', Moscow, 1965) [in Russian].
3. A. G. Zatsepin, P. O. Zavialov, V. V. Kremenetskiy, S. G. Poyarkov, and D. M. Soloviev, "The upper desalinated layer in the Kara Sea," *Oceanology* (Engl. Transl.) **50** (5), 657–667 (2010).
4. A. P. Lisitzin, "Marginal filter of oceans," *Okeanologiya* (Moscow) **34** (5), 735–747 (1994).
5. E. G. Nikiforov and A. O. Shpaikher, *Pattern of the Global Changes in Hydrological Regime of the Arctic Ocean* (Gidrometeoizdat, Leningrad, 1980) [in Russian].
6. V. V. Pelevin, O. I. Abramov, G. G. Karlsen, et al., "Laser sounding of surface waters of Atlantic and European seas," *Opt. Atmos. Okean.* **14** (8), 704–709 (2001).
7. R. Kistler, E. Kalnay, W. Collins, et al., "The NCEP–NCAR 50-year reanalysis: monthly means CD-ROM and documentation," *Bull. Am. Meteorol. Soc.* **82**, 247–268 (2001).
8. W. G. Large, J. C. McWilliams, and S. C. Doney, "Oceanic vertical mixing: a review and a model with a non-local boundary layer parameterization," *Rev. Geophys.* **32**, 363–403 (1994).
9. A. A. Osadchiev and P. O. Zavialov, "Lagrangian model of surface-advected river plume," *Cont. Shelf Res.* **58**, 96–106 (2013).
10. V. Pavlov and S. Pfirman, "Hydrographic structure and variability of the Kara Sea: implications for pollutant distribution," *Deep Sea Res., Part II* **42**, 1369–1390 (1995).
11. J. Smagorinsky, "General circulation experiments with the primitive equation. I. The basic experiment," *Mon. Weather Rev.* **91**, 99–165 (1963).

Translated by O. Ponomareva